# Recent Advances in Sensitivity Analysis with Frequency-Domain Full-Wave EM Solvers

Shirook M. Ali, Natalia K. Nikolova and Mohamed H. Bakr

Department of Electrical and Computer Engineering
McMaster University
Hamilton, Ontario L8S 4K1, CANADA.
Phone +1 905 525 9140 Fax +1 905 523 4407
E-mail: alis5@mcmaster.ca, talia@mcmaster.ca, mbakr@mail.ece.mcmaster.ca

*Abstract* — **This paper introduces recent developments in efficient sensitivity analysis with numerical electromagnetic solvers in the frequency domain. We start by reviewing our original discrete approaches for sensitivity analysis. We then propose and investigate, for the first time, two new discrete approaches which enhance the accuracy of the estimated derivatives. All four introduced approaches are based on the adjoint-variable method and target solvers on structured grids. Discussion and comparison of the accuracy and convergence for the different approaches are also given. Examples include waveguide and printed structures.**

## I. INTRODUCTION

The adjoint-variable sensitivity analysis of 3-D distributed systems has been studied in structural engineering [1], and its use with the finite-element method (FEM) in structural shape design with gradient-based optimizers is a known efficient design approach [2]. Applications with the FEM in electromagnetic problems span problems from eddy currents to high-frequency devices, e.g. [3],[4].

In the implementation of this methodology with other numerical methods, some unsolved problems have been identified. First, time-harmonic electromagnetic (EM) problems lead to complex analysis with complex response functions, while the theory found in [1]-[4], and elsewhere, does not discuss the complex case. Adjoint-network approaches [5] deal with complex problems but their relation to full-wave analysis is not so straightforward. Second, the classical adjoint-variable method assumes that the system matrices are differentiable with respect to the design parameters, and their derivatives are available. In EM analysis, however, the system matrix derivatives—if existing at all—require cumbersome analytical pre-processing and major software changes in the existing full-wave solvers. Besides, methods using structured grids – such as transmission-line matrix (TLM) methods, or finite-difference (FD) methods – produce system matrices, which are not analytical functions of the coordinates of the mesh nodes. Therefore, strictly speaking, they are not differentiable with respect to the shape design parameters.

Here we present a framework of methodologies for EM-based sensitivity analysis where analytical derivatives of the system matrices are not needed. The analytical pre-processing is avoided, and the implementation is made simple and versatile. Our approaches—being adjoint in nature—are efficient, as they compute the system response and all its derivatives with at most two system analyses, regardless of the number of the design parameters.

For the first time, we derive a sensitivity formula in which perturbations relate to the adjoint problem instead of the original problem. This formula has the potential of better accuracy especially when highly nonlinear responses are of interest. We also develop a central adjoint formula which improves the accuracy of the estimated sensitivities even further.

Discussion and comparisons between the presented discrete adjoint techniques are given through a variety of examples including waveguides and printed structures. In addition, conclusions with regard to the accuracy of the presented techniques are made through robust convergence analysis.

We start in Section II by giving a brief review of the mathematical concepts used in sensitivity analysis. Still there, we present our adjoint-based approaches to sensitivity analysis with structured-grid solvers. Practical examples and comparisons are given in Section III. Finally, conclusions are made in Section IV.

## II. MATHEMATICAL FORMULATION

### A. Definitions and Notation

The analysis stage of a design assembles and solves equations, which describe the system. For linear stationary systems,

$$\boldsymbol{A}(\boldsymbol{p})\boldsymbol{x} = \boldsymbol{b}(\boldsymbol{p}), \tag{1}$$

where $\boldsymbol{A} \in \mathbb{C}^{M\times M}$ is the system matrix, $\boldsymbol{x} \in \mathbb{C}^{M\times 1}$ is the state-variable vector, and $\boldsymbol{b} \in \mathbb{C}^{M\times 1}$ is the excitation. In the case of time-harmonic processes, (1) is complex. We denote with $\boldsymbol{p}$ a vector of $N$ shape and/or material design

parameters of the system, which may vary, e.g., to obtain better system performance, or due to technological or environmental factors. We assume that the elements of the design-parameter vector are real-valued. These variations in general affect the system matrix $\boldsymbol{A}$, the excitation vector $\boldsymbol{b}$, and, as a result, the solution as well, i.e., $\boldsymbol{x}(\boldsymbol{p})$. The system output is usually described by a vector of complex-valued responses $\boldsymbol{R}\big(\boldsymbol{x}(\boldsymbol{p})\big)$, e.g., the four *S*-parameters of a two-port microwave network. Its overall performance is often formulated in terms of a single scalar function, $f\big(\boldsymbol{R}(\boldsymbol{p})\big)$, the response function.

The purpose of sensitivity analysis is to describe the rate of change of the response function with each design parameter:

$$\nabla_{\boldsymbol{p}} f \text{ , subject to } \boldsymbol{A}\boldsymbol{x} = \boldsymbol{b}\,, \tag{2}$$

where the gradient is defined as a row operator [1]:

$$\nabla_{\boldsymbol{p}} f = \left[\frac{\partial f}{\partial p_1} \quad \frac{\partial f}{\partial p_2} \quad \cdots \quad \frac{\partial f}{\partial p_N}\right].$$

This information is valuable in optimization, modeling, tolerance and yield analyses.

### *B. Second-order Sensitivity Expression I (AVM-I)*

For a perturbation $\Delta p_i$ in the $i$th parameter, (1) becomes

$$(\boldsymbol{A} + \Delta_i \boldsymbol{A})(\boldsymbol{x} + \Delta_i \boldsymbol{x}) = \boldsymbol{b} + \Delta_i \boldsymbol{b}\,. \tag{3}$$

Here, $\Delta_i$ denotes a variation caused by the perturbation $\Delta p_i$. Simplifying and rearranging (3), we obtain

$$\boldsymbol{A}\Delta_i \boldsymbol{x} + \Delta_i \boldsymbol{A}\cdot\boldsymbol{x} + \Delta_i \boldsymbol{A}\cdot\Delta_i \boldsymbol{x} = \Delta_i \boldsymbol{b}\,. \tag{4}$$

A possible expression for the variation of the state variables is

$$\Delta_i \boldsymbol{x} = \boldsymbol{A}^{-1}\left[\Delta_i \boldsymbol{b} - \Delta_i \boldsymbol{A}\cdot\big(\boldsymbol{x} + \Delta_i \boldsymbol{x}\big)\right] \tag{5}$$

assuming that $\boldsymbol{A}^{-1}$ exists.

This variation is needed to find the derivative of the response function $df/dp_i$, where $f$ can be a complex quantity, $f = f_R + jf_I$. We assume that $f$ is an analytic function of the state variables $\boldsymbol{x} = \boldsymbol{x}_R + j\boldsymbol{x}_I$. In expanded form

$$\begin{aligned}\frac{df}{dp_i} = \frac{\partial f_R}{\partial p_i} + \Bigg(&\frac{\partial f_R}{\partial x_{1R}}\frac{dx_{1R}}{dp_i} + \frac{\partial f_R}{\partial x_{1I}}\frac{dx_{1I}}{dp_i} + \cdots + \frac{\partial f_R}{\partial x_{MR}}\frac{dx_{MR}}{dp_i} \\ &+ \frac{\partial f_R}{\partial x_{MI}}\frac{dx_{MI}}{dp_i}\Bigg) + j\frac{\partial f_I}{\partial p_i} + j\Bigg(\frac{\partial f_I}{\partial x_{1R}}\frac{dx_{1R}}{dp_i} + \frac{\partial f_I}{\partial x_{1I}}\frac{dx_{1I}}{dp_i} \\ &+ \cdots + \frac{\partial f_I}{\partial x_{MR}}\frac{dx_{MR}}{dp_i} + \frac{\partial f_I}{\partial x_{MI}}\frac{dx_{MI}}{dp_i}\Bigg).\end{aligned} \tag{6}$$

Due to the analyticity of $f$, the Cauchy-Riemann relations

$$\frac{\partial f_R}{\partial x_{mR}} = \frac{\partial f_I}{\partial x_{mI}}, \quad \frac{\partial f_R}{\partial x_{mI}} = -\frac{\partial f_I}{\partial x_{mR}}, \quad m = 1,\ldots,M\,, \tag{7}$$

hold. Using (7), we write (6) as

$$\frac{df}{dp_i} = \frac{\partial f}{\partial p_i} + \nabla_{\boldsymbol{x}} f \cdot \frac{d\boldsymbol{x}}{dp_i}\,, \tag{8}$$

where

$$\nabla_{\boldsymbol{x}} f = \nabla_{\boldsymbol{x}_R} f_R - j\nabla_{\boldsymbol{x}_I} f_R = \nabla_{\boldsymbol{x}_R} f_R + j\nabla_{\boldsymbol{x}_R} f_I \text{ , etc.,} \tag{9}$$

and

$$\frac{d\boldsymbol{x}}{dp_i} = \frac{d\boldsymbol{x}_R}{dp_i} + j\frac{d\boldsymbol{x}_I}{dp_i}\,. \tag{10}$$

We approximate (8) as

$$\frac{df}{dp_i} \approx \frac{\partial f}{\partial p_i} + \nabla_{\boldsymbol{x}} f \cdot \frac{\Delta_i \boldsymbol{x}}{\Delta p_i} \tag{11}$$

and substitute (5). The result is the complex sensitivity expression

$$\left(\frac{df}{dp_i}\right)_{AVM\text{-}I} \approx \frac{\partial f}{\partial p_i} + \hat{\boldsymbol{x}}^H \cdot \left[\frac{\Delta_i \boldsymbol{b}}{\Delta p_i} - \frac{\Delta_i \boldsymbol{A}}{\Delta p_i}\big(\boldsymbol{x} + \Delta_i \boldsymbol{x}\big)\right], \quad i = 1,\ldots,N \tag{12}$$

where $\hat{\boldsymbol{x}}$ is the solution of the adjoint system,

$$\boldsymbol{A}^H \hat{\boldsymbol{x}} = [\nabla_{\boldsymbol{x}} f]^H\,. \tag{13}$$

Here, $\boldsymbol{A}^H$ is the Hermitian of the system matrix $\boldsymbol{A}$ in (1), obtained by transposition and conjugation of $\boldsymbol{A}$. $\boldsymbol{A}^H$ is also called adjoint to $\boldsymbol{A}$ in analogy with adjoint operators in functional space analysis. As per (9), the adjoint excitation can be defined as

$$[\nabla_{\boldsymbol{x}} f]^H = \left[\left(\frac{\partial f_R}{\partial x_{1R}} + j\frac{\partial f_R}{\partial x_{1I}}\right)\cdots\left(\frac{\partial f_R}{\partial x_{MR}} + j\frac{\partial f_R}{\partial x_{MI}}\right)\right]^T. \tag{14}$$

If $f$ is a real function [8], then

$$\begin{aligned}\frac{df}{dp_i} \approx \frac{\partial f}{\partial p_i} + \\ \operatorname{Re}\left\{\hat{\boldsymbol{x}}^H \cdot \left[\frac{\Delta_i \boldsymbol{b}}{\Delta p_i} - \frac{\Delta_i \boldsymbol{A}}{\Delta p_i}\big(\boldsymbol{x} + \Delta_i \boldsymbol{x}\big)\right]\right\}, \quad i = 1,\ldots,N\end{aligned} \tag{15}$$

where $\hat{\boldsymbol{x}}$ is the solution of the adjoint problem (13)-(14) with $f = f_R$. Thus, the computational effort involved in the sensitivity calculations of a complex analytic response function is equivalent to that of a real-valued response function. Note that (12) is a generalization of the sensitivity expression developed in [6], [7] to the complex-variable case.

If $f$ is complex but not analytic, then its real and imaginary parts, $f_R$ and $f_I$, have to be treated as two

separate response functions, and two separate adjoint systems of the form (13)-(14) must be solved. Consider for example, a complex response function of the form $f = Z_{in} = 1/x_k$, where $Z_{in}$ is the input impedance at a point excited with a 1-volt and has a corresponding current $x_k$. This response is not differentiable at $x_k = 0$. If the solution is at or very close to this point, we treat $f_R = R_{in} = \mathrm{Re}\{Z_{in}\}$ and $f_I = X_{in} = \mathrm{Im}\{Z_{in}\}$ as two separate real-valued response functions. As a consequence, two adjoint systems must be solved.

Below we summarize the features of the sensitivity formulas (12), (15):

- The adjoint vector $\hat{\boldsymbol{x}}$ requires one additional system analysis (13) (unless *LU* decomposition is used to solve (1), such that the analysis is reduced to forward-backward substitutions [8]). The adjoint problem (13) is perturbation independent.
- The perturbed original system solutions, $\boldsymbol{x} + \Delta_i \boldsymbol{x}$, $i = 1, ..., N$ are perturbation dependent, and thus require $N$ additional system analyses. This drawback is overcome with suitable approximations as explained later.
- No assumptions are made for the magnitudes of the system matrix variations $\Delta_i \boldsymbol{A}$, $i = 1, \ldots, N$; the ratio $\Delta_i \boldsymbol{A} / \Delta p_i$ does not need to represent the respective system matrix derivative with high fidelity, and, in general, it *should not* be considered its finite-difference approximation.
- If, however, $\Delta_i \boldsymbol{A}$, $i = 1, \ldots, N$, are sufficiently small, the second-order terms $\Delta_i \boldsymbol{A} \cdot \Delta_i \boldsymbol{x}$ in (4) can be neglected, thus, leading to the familiar first-order exact sensitivity expression [8]:

$$\frac{df}{dp_i} = \frac{\partial f}{\partial p_i} + \hat{\boldsymbol{x}}^H \cdot \left( \frac{d\boldsymbol{b}}{dp_i} - \frac{d\boldsymbol{A}}{dp_i} \boldsymbol{x} \right), \; i = 1, \ldots, N. \quad (16)$$

The first-order sensitivity expression (16) is applicable with numerical solvers utilizing unstructured grids because such grids allow for a continuous spectrum of values of the design shape parameters. This makes the arising system matrices differentiable with respect to the shape parameters. However, (16) is not suitable for structured-grid algorithms where allowable shape perturbations include only discrete on-grid parameter values. In this case, the second-order sensitivity expression (12) yields better accuracy.

Our technique can be summarized in the following steps:

1. *Parameterization:* specify the set of links $L$ whose corresponding $\boldsymbol{A}$-coefficients are affected by the perturbations $\Delta p_i$, $i = 1, ..., N$.
2. *Original system analysis:* (a) solve the original system (1); (b) store the incident voltages for all the links in the set $L$; (c) store the incident voltages in the observation domain to be used in the computation of the derivatives for the adjoint excitation (14).

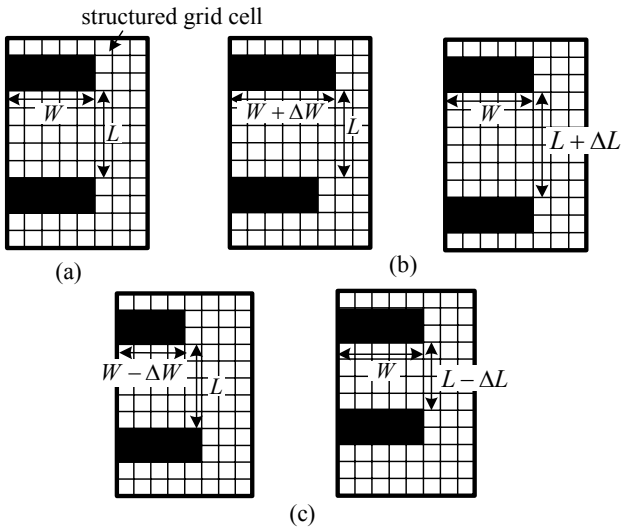


Fig. 1. Discrete on-grid perturbations of the boundaries: (a) the nominal structure; (b) a forward perturbation in *W* and *L;* (c) a backward perturbation in *W* and *L*.

3. *Adjoint analysis:* solve the adjoint problem (13) and store $\boldsymbol{x}$ in the locations that correspond to the set $L$ and the nonzero elements of $\Delta_i \boldsymbol{b}$, $i = 1, ..., N$.
4. *Approximation of the N perturbed problems:* find $\boldsymbol{x} + \Delta_i \boldsymbol{x}$ by performing a mapping between the solutions of the original problem and the perturbed problems for the elements of $\boldsymbol{x}$ that correspond to $L$. See [7] for more details.
5. *Sensitivities estimation:* evaluate the sensitivities using (12) for all $N$ parameters.

### C. Second-order Sensitivity Expression II (AVM-II)

An alternative to (5) is [9]

$$\Delta_i \boldsymbol{x} = (\boldsymbol{A} + \Delta_i \boldsymbol{A})^{-1} \left( \Delta_i \boldsymbol{b} - \Delta_i \boldsymbol{A} \cdot \boldsymbol{x} \right). \quad (17)$$

Repeating all other steps as above , another possible complex sensitivity expression emerges,

$$\left( \frac{df}{dp_i} \right)_{AVM\text{-}II} \approx \frac{\partial f}{\partial p_i} + \hat{\boldsymbol{x}}_i^H \cdot \left( \frac{\Delta_i \boldsymbol{b}}{\Delta p_i} - \frac{\Delta_i \boldsymbol{A}}{\Delta p_i} \boldsymbol{x} \right), \; i = 1, \ldots, N. \quad (18)$$

This time, the unperturbed original problem solution $\boldsymbol{x}$ is used, but the adjoint solution vector $\hat{\boldsymbol{x}}_i$ is perturbation dependent since the complex adjoint problem appears as

$$(\boldsymbol{A} + \Delta_i \boldsymbol{A})^H \hat{\boldsymbol{x}}_i = [\nabla_{\boldsymbol{x}} f]^H, \; i = 1, \ldots, N. \quad (19)$$

Note that neglecting the second-order term in (4) or (17), in this case, too, reduces (18) to the first-order sensitivity formula (16).

This technique can be summarized with the same steps as those of the AVM-II technique. The only difference is that steps 2 (original system analysis) and 3 (adjoint system analysis) are swapped, i.e., perturbations take place in the adjoint system and not the original system. See [9] for more details.

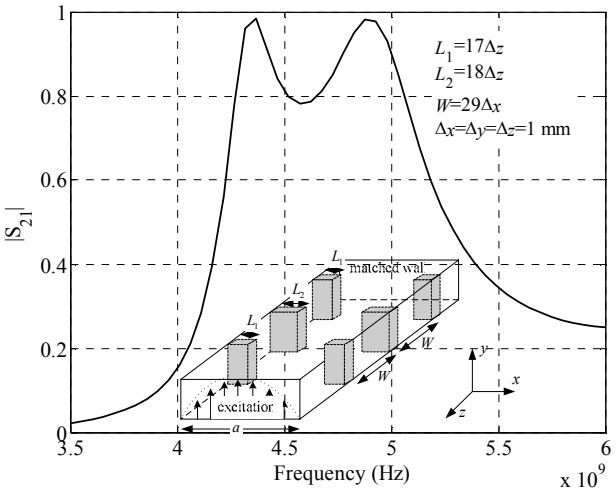


Fig. 2. Insertion loss $|S_{21}|$ of the filter.

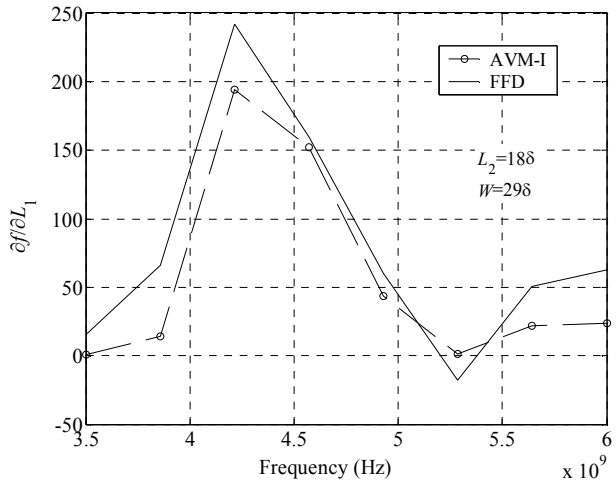


Fig. 3. Derivative of $f$ with respect to $L_1$ vs. frequency.

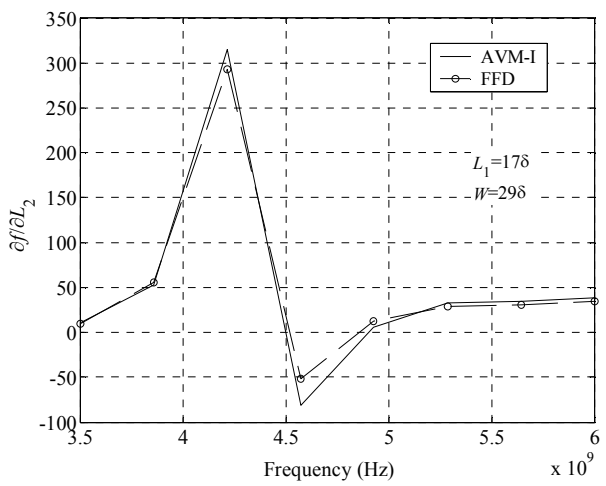


Fig. 4. Derivative of $f$ with respect to $L_2$ vs. frequency.

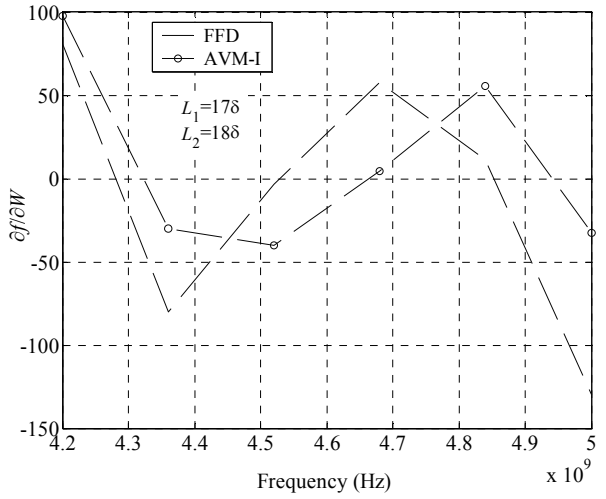


Fig. 5. Derivative of $f$ with respect to $W$ vs. frequency.

The two second-order sensitivity expressions (12) and(18), although theoretically equivalent, exhibit some differences when implemented in practical algorithms. This is mainly due to the self-dependence of the variations in the state variable term in (5), i.e., $\Delta_i \boldsymbol{x}$ appears in both sides of (5) and is hence computed from its own approximation. As a result, we expect the computational error in this term to increase especially with highly nonlinear responses. Notice that, this is not the case in (17) [8].

In general, neither (3)-(12) nor (18)-(19) are actually solved for a perturbation in each of the $N$ parameters. Instead, the values of $\Delta_i \boldsymbol{x}$ are approximated using a simple mapping [6], [7], [9]. The concept is based on the perturbation theory [10], and it can be implemented for conducting and dielectric parameters.

### *D. Central Approaches with Sensitivity Expressions*

As mentioned earlier, with structured grid solvers, allowable perturbations are limited to multiples of the grid size in the respective direction. For example, consider the structure in Fig. 1. The dark rectangles may be either conducting or dielectric objects. The nominal design of this structure is shown in Fig. 1 (a) where $\boldsymbol{p} = [L \;\; W]^T$ is the vector of design parameters. AVM-I (12) can be used when perturbations in the forward direction [see Fig. 1(b)] take place in the original problem. It can also be used when perturbations are in the backward direction [see Fig. 1(c)]. The sensitivity results obtained from the forward and backward perturbations are somewhat different especially when the response $\boldsymbol{R}$ is a highly nonlinear function of $\boldsymbol{p}$. The same forward, backward and central approaches can be applied with the AVM-II (18).

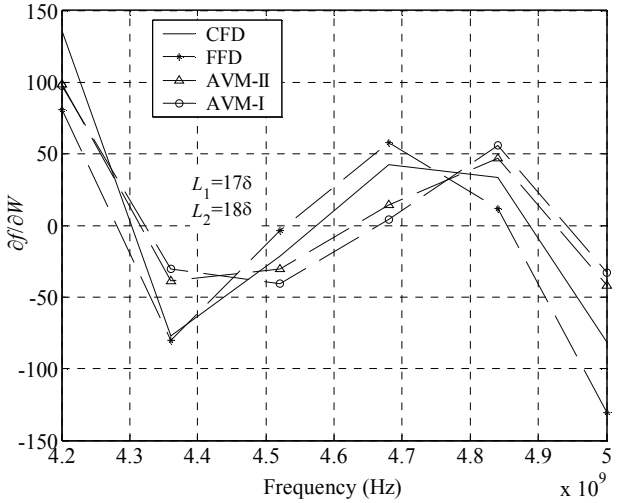


Fig. 6. A Comparison between response level sensitivities and adjoint-based sensitivities.

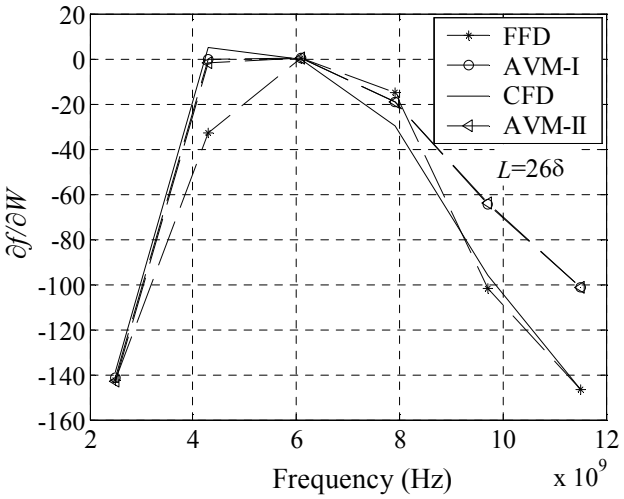


Fig. 8. Derivative of $f$ with respect to $W$ for the printed filter.

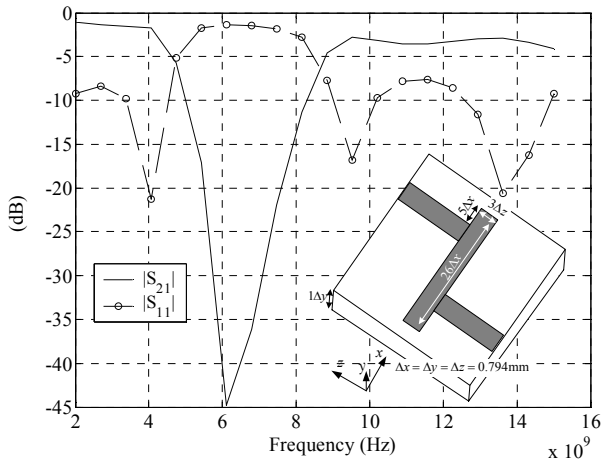


Fig. 7. Reflection and transmission coefficients of the printed filter.

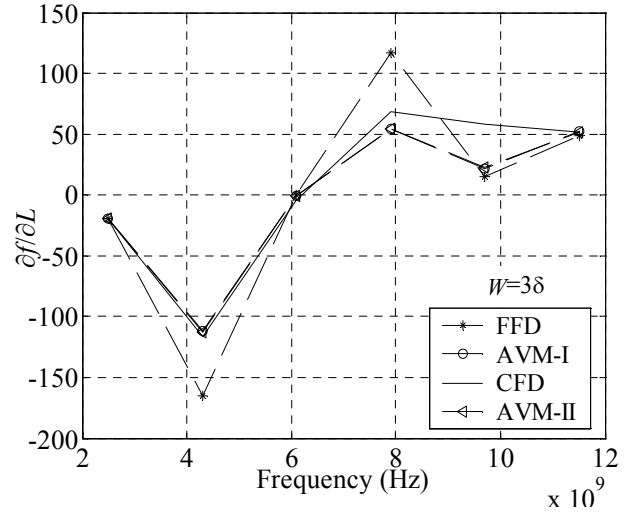


Fig. 9. Derivative of $f$ with respect to $L$ for the printed filter.

Major improvement in the accuracy can be achieved using the central adjoint approach [11]. The central formula (CAVM-I) combines the solutions of the forward and backward sensitivity expressions. Its complex form is

$$\left(\frac{df}{dp_i}\right)_{CAVM\text{-}I} \simeq \frac{\partial f}{\partial p_i} + \hat{\boldsymbol{x}}^H \cdot \left\{ \frac{\Delta_i \boldsymbol{b}^+ + \Delta_i \boldsymbol{b}^-}{2\Delta p_i} - \frac{\Delta_i \boldsymbol{A}^+ \boldsymbol{x}_i^+ + \Delta_i \boldsymbol{A}^- \boldsymbol{x}_i^-}{2\Delta p_i} \right\}, \quad i = 1, \ldots, N. \tag{20}$$

In (20), the plus sign (+) refers to a perturbation in the forward direction and the minus sign (−) refers to that in the backward direction.

Since we have observed that the computational error is, in fact, reduced with AVM-II (18), we consider here the same forward/backward procedure and derive a central formula for AVM-II (CAVM-II) as well:

$$\left(\frac{df}{dp_i}\right)_{CAVM\text{-}II} \simeq \frac{\partial f}{\partial p_i} + \frac{\hat{\boldsymbol{x}}_i^{+H} \Delta_i \boldsymbol{b}^+ + \hat{\boldsymbol{x}}_i^{-H} \Delta_i \boldsymbol{b}^-}{2\Delta p_i} - \frac{\hat{\boldsymbol{x}}_i^{+H} \Delta_i \boldsymbol{A}^+ + \hat{\boldsymbol{x}}_i^{-H} \Delta_i \boldsymbol{A}^-}{2\Delta p_i} \cdot \boldsymbol{x}, \quad i = 1, \ldots, N. \tag{21}$$

The improvement in the accuracy due to the central formulas (20) and (21) is, in some cases, very significant over the sensitivity results produced by formulas (12) and (18). Note however, that the computational load is the same for all four approaches.

## III. Examples and Comparisons

In this section, we show sensitivity results computed with our adjoint techniques through a variety of different structures. The structures are chosen so that: (i) different types of perturbations are possible, i.e., volumetric

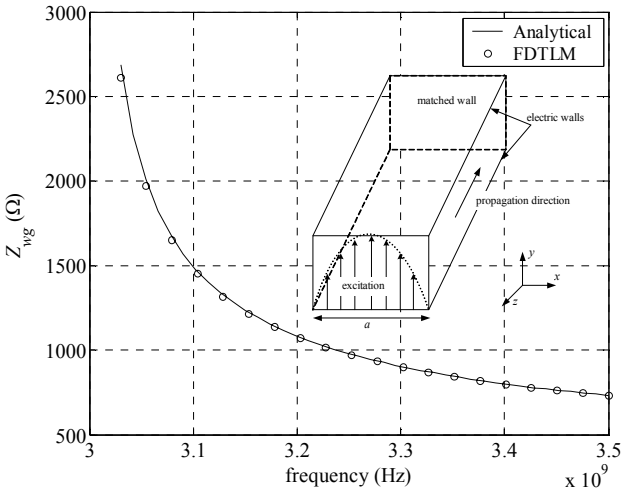


Fig. 10. The wave impedance of the waveguide vs. frequency at $a = 5$ cm.

perturbations, as in waveguide structures, as well as metallic surface perturbations in printed structures; and (ii) the selected response is a highly nonlinear function of its design parameters.

The adjoint results are compared with those computed using classical finite differences at the level of the response or with sensitivity results calculated analytically whenever available.

The structures are simulated using an in - house simulator based on the frequency-domain transmission line method (FDTLM) [12]. A uniform discretization grid is used, i.e., $\Delta x = \Delta y = \Delta z = \delta$ and $\Delta p_i = \delta$.

### A. Results with AVM-I

Using AVM-I, we compute response sensitivities for the double-resonator filter shown in the inset of Fig. 2 for a range of frequencies. The filter is analyzed for its dominant mode and thus the problem reduces to two dimensions. The computational size of the problem is $30 \times 1 \times 120\ \delta$. The filter is excited with a uniform half sine-wave at its input port. The input and output ports are matched to absorb the reflected waves.

The response function is defined as $f = |S_{21}|$, where $S_{21}$ is the transmission coefficient for the filter. The response is shown in Fig. 2. The vector of design parameters is $\boldsymbol{p} = [L_1 \ L_2 \ W]^T$, where $L_2$ and $L_1$ are the lengths of the middle and side septa, respectively. $W$ is the separation between the septa.

For comparison, the sensitivities are also computed using forward finite differences (FFD) directly at the level of the response [Figs. 3, 4, and 5].

TABLE 1
COMPARISON BETWEEN THE DERIVATIVES FROM THE CONVERGENCE ANALYSIS.

| δ | → 0 | λ/80 | λ/20 | λ/10 |
|---|---|---|---|---|
| • analytical | | -1.244 | | |
| • AVM-I | -1.2471 | -1.2481 | -1.2530 | -1.2550 |
| • CAVM-I | -1.2470 | -1.2480 | -1.2510 | -1.2520 |
| • AVM-II | -1.2459 | -1.2471 | -1.2500 | -1.2513 |
| • CAVM-II | -1.2455 | -1.2460 | -1.2481 | -1.2501 |

### B. Results with AVM-II and Comparisons with AVM-I

#### 1) Double-resonator Filter

For the same double-resonator filter shown in Fig. 2, we compute the sensitivity results for $f = |S_{21}|$ with respect to $W$ using AVM-II. The results are compared with those produced with AVM-I from Section III.A as shown in Fig. 6. For better comparison of the accuracies of AVM I and II, we compute a reference sensitivity using the second-order central finite differences (CFD) at the level of the response. Notice that this is a highly nonlinear response function. Even with a relatively fine grid, the FFD and CFD sensitivities disagree. Results computed with AVM-II show acceptable accuracy compared to the reference CFD and a noticeable improvement over those computed using AVM-I.

#### 2) Microstrip Low-pass Filter

With this example, the perturbations are of infinitesimal surface type. The relative permittivity of the substrate is $\varepsilon_r = 2.2$. The total size of the simulated problem is $43 \times 37 \times 7\ \delta$. We excite the structure with a voltage source applied uniformly underneath the strip-line at port 1 in the $y$-direction.

We compute the sensitivities for the printed low-pass filter shown in the inset of Fig. 7. The response function is the squared modulus of the transmission coefficient of the filter, i.e., $f = |S_{21}|^2$ [see Fig. 7]. The vector of design parameters is $\boldsymbol{p} = [L \ W]^T$, where $L$ is the length of the resonating element and $W$ is its width.

The sensitivities are computed with respect to changes in the vector of design parameters $\boldsymbol{p} = [L \ W]^T$ using both AVM I and II. The computed results are compared with first and second-order finite difference estimates at the level of the response as shown in Figs. 8 and 9.

As seen from this example, the difference between the adjoint-based sensitivities is small. This is also true for the results from the previous example when the sensitivities are computed with respect to changes in $L_1$ and $L_2$ [see Fig. 2]. It is thus difficult to conclude with certainty which approach provides better accuracy. Therefore, more detailed comparison based on convergence analysis is needed.

### C. Convergence Analysis

In this section, we test the accuracy of our adjoint approaches presented in Sections II.B to II.D through a convergence test, i.e., we compute the sensitivity of a response function using each of the four approaches at a given design, and compare their accuracy as the grid size $\delta$ becomes smaller. For this test to be accurate, we choose a response function that is analytically available, and therefore, its derivative can be calculated analytically. We consider the wave impedance ( $f = Z_{wg}$ ) of a hollow rectangular waveguide [see the inset of Fig. 10]. The computed adjoint derivatives are compared to the analytical derivative.

The response is calculated analytically using the well-known formula for $Z_{wg}$ as a function of the waveguide cross-section dimensions and the frequency [13]. The response function is also computed using our FDTLM simulator as shown in Fig. 10.

The convergence analysis is executed at a given design point in the highly nonlinear region of the response function [see Fig. 10]. For example, consider the design where the waveguide width is $a = 5$ cm and the frequency is 3.05 GHz. For this design, the four adjoint sensitivities are computed for different uniform discretization grid of the TLM simulator, i.e., at $\delta = \lambda/10$ to $\delta = \lambda/80$, where $\lambda$ is the wavelength. The derivatives for a finer grid at $\delta \to 0$ are estimated using Matlab's [14] extrapolating functions. The results are given in Table 1.

The results show that all four approaches tend to converge to the analytical value of the derivative as the grid size $\delta$ becomes finer. This is due to the dependence of the field approximation in the perturbed problems [7] on the grid size. It can also be observed that the results produced with CAVM-II give the best outcome for any grid size compared to the other results. The CAVM-II results also show a smoother convergence than the other approaches. Our interpretation to this outcome is: (i) the numerical error produced by the sensitivity expression II (18) is less than that of sensitivity expression I (12); and (ii) the CAVM, in general, preserves the advantages of the second-order term $\Delta_i \boldsymbol{A} \cdot \Delta_i \boldsymbol{x}$ since it takes into account both forward and backward perturbations in the design parameter. With the CAVM-II, we merge the above advantages and obtain the best results.

It is also observed that the difference between the AVM-I and CAVM-I derivatives at finer grid sizes is small. However, we would like to point out that larger differences are expected with responses that are functions of shape design parameters in which the electromagnetic field is singular at the locations of the perturbed boundaries [11]. There are no field singularities in our waveguide example as the field smoothly decays to zero at the edge of the electric conducting walls of the waveguide. Therefore, the field variations between the approximated perturbed solution and that of the original unperturbed problem are not very different. Hence, the difference in the corresponding derivatives is not so pronounced.

## IV. CONCLUSIONS

We present a framework of approaches for feasible and versatile adjoint-based sensitivity analysis with frequency-domain structured-grid electromagnetic solvers. For the first time, we present two new adjoint-based approaches that further improve the accuracy of the estimated sensitivities. All approaches are easy to implement with existing solvers and do not require solver-dependent analytical preprocessing. They provide cheap and accurate gradient information, which is valuable in a number of CAD applications such as optimization, modeling, and tolerance analysis.

We also test and compare the accuracy of our presented approaches through the computed sensitivities of a variety of structures and through robust convergence analysis. Conclusions are made based on comparisons with finite difference response-level sensitivities and with analytical derivatives.

## REFERENCES

[1] E. J. Haug, K. K. Choi and V. Komkov, *Design Sensitivity Analysis of Structural Systems*. Orlando: Academic Press Inc., 1986.

[2] A. D. Belegundu and T. R. Chandrupatla, *Optimization Concepts and Applications in Engineering*. Upper Saddle River, NJ: Prentice Hall, 1999.

[3] I.-H. Park, I.-G. Kwak, H.-B. Lee, S.-Y. Hahn and K.-S. Lee, "Design sensitivity analysis for transient eddy current problems using finite element discretization and adjoint variable method," *IEEE Trans. Mag.*, vol. 32, pp. 1242-1245, May 1996.

[4] J.P. Webb, "Design sensitivity of frequency response in 3-D finite-element analysis of microwave devices," *IEEE Trans. Mag.*, vol. 38, No. 2, pp. 1109-1112, Mar. 2002.

[5] J. W. Bandler, Q.-J. Zhang and R. M. Biernacki, "A unified theory for frequency-domain simulation and sensitivity analysis of linear and nonlinear circuits," *IEEE Trans. MTT*, vol. 36, pp. 1661-1669, Dec. 1988.

[6] M. H. Bakr and N. K. Nikolova, "An adjoint variable method for frequency domain TLM problems with conducting boundaries," *IEEE Microwave Wireless Components Lett.*, vol. 13, pp. 408-410, Sep. 2003.

[7] S. M. Ali, N. K. Nikolova and M. H. Bakr, "Sensitivity analysis with full-wave EM solvers based on structured grids," *IEEE Trans. Mag.*, vol. 40, No. 3, pp. 1521-1529, May, 2004.

[8] N. K. Nikolova, J. W. Bandler and M. H. Bakr, "Adjoint techniques for sensitivity analysis in high-frequency structure CAD," *IEEE Trans. MTT*, vol. 52, No. 1, pp. 403-419, Jan. 2004.

[9] S. M. Ali, N. K. Nikolova, and M. H. Bakr, " Sensitivity analysis and optimization utilizing an approximate auxiliary problem," *IEEE/URSI Int. Symposium on Antennas and Propagation*, June 2004 (Monterey, CA), vol.1, pp. 1118-1121.

[10] R. F. Harrington, *Time-Harmonic Electromagnetic Fields*. New York: McGraw-Hill book company, Inc., 1961.

[11] S. M. Ali, N. K. Nikolova, and M. H. Bakr, "Central adjoint variable method for sensitivity analysis with structured grid electromagnetic solvers," *IEEE Trans. Mag*., pp. 1969-1971, July, 2004.
[12] D. Johns and C. Christopoulos, "New frequency-domain TLM method for the numerical solution of steady-state electromagnetic problems," *IEE Proc. Sci Meas. Technol.*, vol. 141, pp. 310-316, 1994.
[13] D. M. Pozar, *Microwave Engineering*. New York: Addison-Wesley Publishing Company, Inc., 1993.
[14] MATLAB (2000) Version 6.0, MathWorks, Inc., 3 Apple Hill Drive, Natick MA 01760-2098.

**Shirook M. Ali** received the B.Sc. degree from University of Baghdad, Iraq, in 1993, and the M.Sc. degree from Jordan University of Science and Technology, Jordan, in 1999. She is currently working toward her Ph.D. at McMaster University, Canada. Her research interests include computational electro-magnetics, optimization, and CAD methods for high-frequency structures and antennas.

**Natalia K. Nikolova** received the Dipl. Eng. degree from the Technical University of Varna, Bulgaria, in 1989, and the Ph.D. degree from the University of Electro-Communications, Tokyo, Japan, in 1997. From 1998 to 1999, she held a Postdoctoral Fellowship of the Natural Sciences and Engineering Research Council of Canada (NSERC), during which time she was initially with the Microwave and Electromagnetics Laboratory, DalTech, Dalhousie University, Halifax, Canada, and, later, for a year, with the Simulation Optimization Systems Research Laboratory, McMaster University, Hamilton, ON, Canada. In July 1999, she joined the Department of Electrical and Computer Engineering, McMaster University, where she is currently an Associate Professor. Her research interests include theoretical and computational electromagnetism, high-frequency analysis techniques, as well as CAD methods for high-frequency structures and antennas.

Dr. Nikolova currently holds a University Faculty Award of NSERC, which she received in 2000, and which was renewed in 2003.

**Mohamed H. Bakr** received a B.Sc. degree in Electronics and Communications Engineering from Cairo University, Egypt in 1992 with distinction (honors). In June 1996, he received a Master's degree in Engineering Mathematics from Cairo University. In 1997, he was a student intern with Optimization Systems Associates (OSA), inc. From 1998 to 2000 , he worked as a research assistant with the Simulation Optimization Systems (SOS) research laboratory, McMaster University, Hamilton, Ontario, Canada. He earned the Ph.D. degree in September 2000 from the Department of Electrical and Computer Engineering, McMaster University. In November 2000, he joined the Computational Electromagnetics Research Laboratory (CERL), University of Victoria, Victoria, Canada as an NSERC Post Doctoral Fellow. Dr. Bakr is a recipient of a 2003 Premier's Research Excellence Award (PREA) from the province of Ontario, Canada. His research areas of interest include optimization methods, computer-aided design and modeling of microwave circuits, neural network applications, smart analysis of microwave circuits and efficient optimization using time/frequency domain methods. He is currently an Assistant Professor with the Department of Electrical and Computer Engineering, McMaster University.